Dynamical Phase Transitions and Instabilities in Open Atomic Many-Body Systems

Sebastian Diehl,[1,2] Andrea Tomadin,[2,3] Andrea Micheli,[1,2] Rosario Fazio,[3] and Peter Zoller[1,2]
[1]*Institute for Theoretical Physics, University of Innsbruck, Technikerstrasse 25, A-6020 Innsbruck, Austria*
[2]*Institute for Quantum Optics and Quantum Information of the Austrian Academy of Sciences, A-6020 Innsbruck, Austria*
[3]*NEST, Scuola Normale Superiore and Istituto Nanoscienze—CNR, Pisa, Italy*
(Received 10 March 2010; revised manuscript received 17 May 2010; published 1 July 2010)

We discuss an open driven-dissipative many-body system, in which the competition of unitary Hamiltonian and dissipative Liouvillian dynamics leads to a nonequilibrium phase transition. It shares features of a quantum phase transition in that it is interaction driven, and of a classical phase transition, in that the ordered phase is continuously connected to a thermal state. We characterize the phase diagram and the critical behavior at the phase transition approached as a function of time. We find a novel fluctuation induced dynamical instability, which occurs at long wavelength as a consequence of a subtle dissipative renormalization effect on the speed of sound.

DOI: 10.1103/PhysRevLett.105.015702 PACS numbers: 64.70.Tg, 03.75.Kk, 67.85.Hj

Experiments with cold atoms provide a unique setting to study nonequilibrium phenomena and dynamics, both in closed systems but also for (driven) open quantum dynamics. This relies on the ability to control the many-body dynamics and to prepare initial states far from the ground state. For closed systems we have seen a plethora of studies of quench dynamics [1,2], thermalization [3,4], and transport [5], and also dynamical studies of crossing in a finite time quantum critical points in the spirit of the Kibble-Zurek mechanism [6,7]. On the other hand, systems of cold atoms can be driven by external (light) fields and coupled to dissipative baths, thus realizing driven open quantum systems. As familiar, e.g., from the quantum optics of the laser, the steady state of such a system (if it exists) is characterized by a dynamical equilibrium between pumping and dissipation, and can exhibit various nonequilibrium phases and phase transitions [8,9] as function of external control parameters. In the present work we will study such scenarios for quantum degenerate gases. Our emphasis is on understanding quantum phases and dynamical phase transitions of cold atoms as an interacting many-body condensed matter system far from equilibrium. In particular, we will establish several observable aspects which are uniquely tied to the nonequilibrium nature of the problem.

For a many-body system in thermodynamic equilibrium the competition of two noncommuting parts of a microscopic Hamiltonian $H = H_1 + gH_2$ manifests itself as a quantum phase transition (QPT), if the ground states for $g \ll g_c$ and $g \gg g_c$ have different symmetries [10]. For temperature $T = 0$ the critical value g_c then separates two distinct quantum phases, while for finite temperature this defines a quantum critical region around g_c in a T vs g phase diagram. A seminal example in the context of cold atoms in optical lattices is the superfluid-Mott insulator transition in the Bose-Hubbard (BH) model, with Hamiltonian

$$H = -J\sum_{\langle \ell,\ell' \rangle} b_\ell^\dagger b_{\ell'} - \mu \sum_\ell \hat{n}_\ell + \frac{1}{2}U\sum_\ell \hat{n}_\ell(\hat{n}_\ell - 1), \quad (1)$$

with b_ℓ bosonic operators annihilating a particle on site ℓ, $\hat{n}_\ell = b_\ell^\dagger b_\ell$ number operators, J the hopping amplitude, and U the onsite interaction strength. For a given chemical potential μ, chosen to fix a mean particle density n, the critical coupling strength $g_c = (U/Jz)_c$ separates a superfluid $Jz \gg U$ from a Mott insulator regime $Jz \ll U$ (z the lattice coordination number).

In contrast, we consider a nonequilibrium situation in which the competition of microscopic quantum mechanical operators results from Hamiltonian and dissipative dynamics. We study a cold atom evolution described by a master equation for the density operator

$$\partial_t \rho = -i[H, \rho] + \mathcal{L}[\rho],$$
$$\mathcal{L}[\rho] = \frac{1}{2}\kappa \sum_{\langle \ell,\ell' \rangle} (2c_{\ell\ell'}\rho c_{\ell\ell'}^\dagger - c_{\ell\ell'}^\dagger c_{\ell\ell'}\rho - \rho c_{\ell\ell'}^\dagger c_{\ell\ell'}), \quad (2)$$

where $c_{\ell\ell'} = (b_\ell^\dagger + b_{\ell'}^\dagger)(b_\ell - b_{\ell'})$ are "jump operators" acting on adjacent sites $\langle \ell, \ell' \rangle$. The energy scale κ is the dissipative rate. As shown in [11], such dissipative reservoir couplings are obtained in a setup where laser driven atoms are coupled to a phonon bath provided by a second condensate. For $U = 0$ this dissipation drives the system to a dynamical equilibrium independent of the initial state [11] given by the *pure many-body state* $\rho_{ss} = |\mathrm{BEC}\rangle\langle\mathrm{BEC}|$ representing a Bose Einstein condensate. From an atomic physics point of view this is remarkable, as typical decoherence mechanisms, such as spontaneous emission, will destroy long range order, whereas here the bath coupling is engineered to suppress phase fluctuations. This can be understood in momentum space, where the annihilation part of $c_{\ell\ell'}$ reads $\sum_\lambda (1 - \exp(i\mathbf{q}_\lambda a))b_\mathbf{q}$, with λ the reciprocal lattice directions and a the lattice constant. $c_{\ell\ell'}$ thus feature a (unique) dissipative zero mode at $\mathbf{q} = 0$—a many-body "dark state" $|\mathrm{BEC}\rangle \sim b_{\mathbf{q}=0}^{\dagger N}|\mathrm{vac}\rangle$ decoupled from the bath, into which the system is driven for long wait times. The dynamics behind Eq. (3) can be understood as a "dark state laser cooling" [12] into a condensate.

Turning on an interaction measured by $u = U/(4\kappa z)$ provides a Hamiltonian term in (3) which is incompatible with kinetic energy and dissipation. This competition leads to novel dynamical equilibria which cannot be understood as thermodynamic equilibrium states. They are summarized in the steady state phase diagram in Fig. 1. Most prominently, it features a strong coupling phase transition as a function of u. The transition shares features of a QPT in that it is interaction driven, and of a classical phase transition in that the ordered phase terminates in a mixed state. This contrasts equilibrium QPTs, in which the system remains in a pure zero temperature state across the transition.

We show the existence of a novel dynamical instability that covers an extensive domain of the phase diagram. Again, this is a nonequilibrium effect, since in equilibrium, finite momentum excitations carry positive kinetic energy ruling out dynamical instabilities. It persists at arbitrarily weak interaction parameters Un. This is in marked contrast to the "classical" dynamical instabilities of condensates in boosted lattices [13,14] or in exciton-polariton systems [15], which are triggered by external parameter tuning beyond finite critical values.

Our scenario shares analogies with the well-known dissipation induced phase transition to a superconductor in Josephson junction arrays [16], in which similarly phase fluctuations are suppressed via the coupling to a dissipative bath. We stress, however, that the latter system is in global thermal equilibrium, thus not displaying the nonequilibrium aspects highlighted here.

Nonlinear mean field master equation.—To solve the master equation we developed a generalized Gutzwiller approach, expected to hold in sufficiently high spatial dimension, which allows us to include mixed states. This is implemented by a product ansatz $\rho = \bigotimes_\ell \rho_\ell$, with the reduced local density operators $\rho_\ell = \mathrm{Tr}_{\neq \ell}\rho$. The equation of motion (EOM) reads

$$\partial_t \rho_\ell = -i[h_\ell, \rho_\ell] + \mathcal{L}_\ell[\rho_\ell], \tag{3}$$

with the local Hamiltonian $h_\ell = -J\sum_{\langle \ell' | \ell \rangle}(\langle b_{\ell'}\rangle b_\ell^\dagger + \langle b_{\ell'}^\dagger \rangle b_\ell) - \mu \hat{n}_\ell + \frac{1}{2} U \hat{n}_\ell(\hat{n}_\ell - 1)$ and a Liouvillian of the form $\mathcal{L}_\ell[\rho_\ell] = \kappa \sum_{\langle \ell' | \ell \rangle} \sum_{r,s=1}^4 \Gamma_{\ell'}^{rs}[2A_\ell^r \rho_\ell A_\ell^{s\dagger} - A_\ell^{s\dagger} A_\ell^r \rho_\ell - \rho_\ell A_\ell^{s\dagger} A_\ell^r]$. The Liouvillian is constructed with the vector of operators $\mathbf{A}_\ell = (1, b_\ell^\dagger, b_\ell, \hat{n}_\ell)$ and the matrix of correlation functions $\Gamma_\ell^{r,s} = \sigma^r \sigma^s \mathrm{Tr}_\ell A_\ell^{(5-s)\dagger} A_\ell^{(5-r)} \rho_\ell$, for $\sigma = (-1, -1, 1, 1)$. The ρ-dependent correlation matrix makes the master equation *nonlinear* in ρ_ℓ.

Dynamical quantum phase transition.—At $U = 0$ a steady state solution of Eq. (3) is given by the pure state $\rho_\ell^{(c)} = |\Psi\rangle\langle\Psi|$ for any ℓ together with the choice $\mu = -Jz$, where $|\Psi\rangle$ is a coherent state of parameter $ne^{i\theta}$ for any phase θ [17]. In order to understand the effect of a finite interaction U, we apply the rotating-frame transformation $\hat{V}(U) = \exp[iU\hat{n}_\ell(\hat{n}_\ell - 1)t]$ to Eq. (3). This removes the interaction term from the unitary evolution, but the annihilation operators become $\hat{V} b_\ell \hat{V}^{-1} = \sum_m \exp(imUt)|m\rangle_\ell \langle m| b_\ell$. The effect of a finite U is thus to rotate the phase of each Fock state differently, leading to dephasing of the coherent state $\rho_\ell^{(c)}$. Hence, for strong enough U, off-diagonal order is suppressed completely and the density matrix becomes diagonal. In this case Eq. (3) reduces precisely to the master equation for a system of bosons coupled to a thermal reservoir with occupation n [17], whose solution is a mixed diagonal thermal state $\rho^{(t)}$. Interestingly, this state is thermal-like; however, the role of the thermal bath is played by the system itself.

We substantiate the discussion above with the numerical integration of the EOM (3) for a homogeneous system (we drop the index ℓ). The system is initially in the coherent state and the condensate fraction $|\psi|^2/n$, where $\psi = \langle b \rangle$, decreases in time depending on the value of the interaction strength U. The result is a continuous transition from the coherent state $\rho^{(c)}$ to the thermal state $\rho^{(t)}$, shown in Fig. 2. The boundary between the thermal and the condensed phase with varying J, n is shown in Fig. 1.

The transition is a smooth crossover for any finite time, but for $t \to \infty$ a sharp nonanalytic point indicating a second order phase transition develops. In the universal vicinity of the critical point, $1/\kappa t$ may be viewed as an irrelevant coupling in the sense of the renormalization group. We may use this attractive irrelevant direction to extract the critical exponent α for the order parameter from the scaling solution $|\psi(t)| \propto (\kappa t)^{-\alpha}$. In the inset of Fig. 2 we plot $\alpha(t) = d\log(\psi)/d\log(1/t)$ and read off the critical exponent $\alpha = 0.5$ in the scaling regime, which is an expected result given the mean field nature of the Gutzwiller ansatz. We emphasize that following the relaxation dynamics of the condensate fraction for critical system parameters gives an experimental handle for the measurement of α.

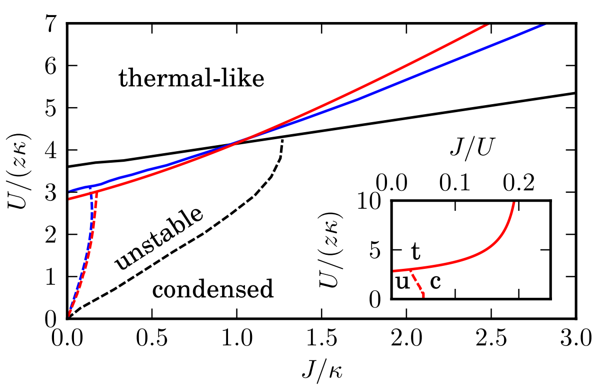

FIG. 1 (color online). Nonequilibrium phase diagram for the model in Eq. (3). The solid lines indicate the border of the dynamical quantum phase transition from a condensed to a homogeneous thermal steady state. The dashed lines delimit the region where the condensed state is stable. The black (blue) lines are the numerical results corresponding to average density $n = 1.0$ ($n = 0.1$). The red line corresponds to the analytical results for $n = 0.1$.

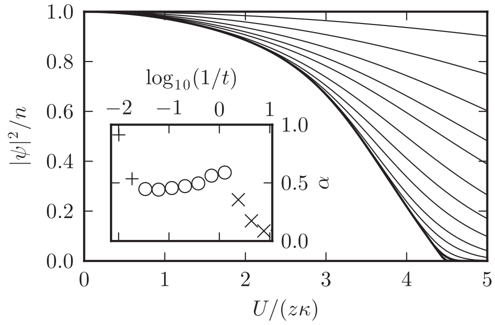

FIG. 2. Stroboscopic plot of the time evolution of the condensate fraction as a function of the interaction strength U, for $J = 1.5\kappa$ and $n = 1$. For large times it converges to the lower thick solid line. The critical point is $U_c \simeq 4.5\kappa z$. Inset: Near critical evolution for $J = 0$, $n = 1$, and $U \lesssim U_c$. The early exponential decay ($\times$) is followed by a scaling regime ($\bigcirc$) with exponent $\alpha \simeq 0.5$. The final exponential runaway ($+$) is due to a small deviation from the critical point.

Low-density limit.—In the low-density limit $n \ll 1$ we obtain an analytical understanding of the time evolution based on the observation that the six correlation functions ψ, $\langle b_\ell^2\rangle$, $\langle b_\ell^\dagger b_\ell^2\rangle$, and complex conjugates, form a closed (nonlinear) subset which decouples from the *a priori* infinite hierarchy of normal ordered correlation functions $\langle b_\ell^{\dagger n} b_\ell^m\rangle$. We first use this result to obtain analytically the critical exponent α discussed above. For a homogeneous system with $J = 0$ the EOMs read

$$\begin{aligned}\partial_t\psi &= i\mu\psi + (-iU + 4\kappa)\langle b^\dagger b^2\rangle - 4\kappa\psi^*\langle b^2\rangle,\\ \partial_t\langle b^\dagger b^2\rangle &= 8n\kappa\psi + (-iU + i\mu - 8\kappa)\langle b^\dagger b^2\rangle,\\ \partial_t\langle b^2\rangle &= (-iU + 2i\mu - 8\kappa)\langle b^2\rangle + 8\kappa\psi^2.\end{aligned} \tag{4}$$

The structure of the equations suggest that $\langle b^2\rangle$ decays much faster than the other correlations for $U = U_c$, so that we may take $\partial_t\langle b^2\rangle = 0$ and hence $\langle b^2\rangle \propto \psi^2$. At the critical point the two linear contributions to $\partial_t\psi$ vanish due to the zero mass eigenvalue at criticality and $\partial_t\psi \propto \kappa\psi^2\psi^*$. It follows that $|\psi| \simeq 1/(4\sqrt{\kappa t})$ in agreement with the numerical result in Fig. 2.

To study the interaction induced depletion of the condensate fraction, it is convenient to use "connected" correlation functions, built with the fluctuation operator $\delta b = b - \psi_0$. Here ψ_0 is the constant value of the order parameter in the steady state, and $\langle\delta b\rangle = 0$. From (4) we obtain a closed *linear* system of EOMs, if ψ_0 is considered as a parameter, determined self-consistently from the identity $n = \langle\delta b^\dagger\delta b\rangle + |\psi_0|^2$. The value of the chemical potential is fixed to remove the driving terms in the equations for $\langle\delta b\rangle$, leading to $\mu = nU$. This is an equilibrium condition similar to the vanishing of the mass of the Goldstone mode in a thermodynamic equilibrium system with spontaneous symmetry breaking. The solution of the equations in steady state yields the condensate fraction

$$\frac{|\psi_0|^2}{n} = 1 - \frac{2u^2(1 + (j+u)^2)}{1 + u^2 + j(8u + 6j(1 + 2u^2) + 24j^2u + 8j^3)}, \tag{5}$$

with dimensionless variable $j = J/(4\kappa)$. Equation (5) reduces to the simple quadratic expression $1 - 2u^2$ in the limit of zero hopping, with the critical point $U_c(J = 0) = 4\kappa z/\sqrt{2}$. The phase boundary, obtained by setting $\psi_0 = 0$ in Eq. (5), reads $u_c = j + \sqrt{1/2 + 2j^2}$. Figure 1 shows that these compact analytical results (solid red line) match the full numerics for small densities (solid blue line), and also explain the qualitative features of the phase boundary for large densities. We note the absence of distinct commensurability effects, e.g., $n = 1$, tied to the fact that the interaction also plays the role of heating.

Dynamical instability.—Numerically integrating the full EOM (3) with site dependence (in one dimension for simplicity), we observe a dynamical instability, manifesting itself at late times in a long wavelength density wave with growing amplitude. Numerical linearization of Eq. (3) around the homogeneous steady state allows us to draw a phase border for the unstable phase (see Fig. 1). The instability is cured by the increase of hopping J, which is associated to an operator compatible with dissipation κ. Furthermore, we note that the thermal state is always dynamically stable against long wavelength perturbations.

The origin of this instability is intriguing and we discuss it analytically within the low-density limit introduced above. We linearize in time the EOM (3), writing the generic connected correlation function as $\langle\hat{O}_\ell\rangle(t) = \langle\hat{O}_\ell\rangle_0 + \delta\langle\hat{O}_\ell\rangle(t)$, where $\langle\hat{O}_\ell\rangle_0$ is evaluated on the homogeneous steady state of the system. The EOM for the time- and space-dependent fluctuations is then Fourier transformed, resulting in a 7×7 matrix evolution equation $\partial_t\delta\Phi_{\mathbf{q}} = M\delta\Phi_{\mathbf{q}}$ for the correlation functions $\Phi_{\mathbf{q}} = (\langle\delta b\rangle_{\mathbf{q}}, \langle\delta b^\dagger\rangle_{\mathbf{q}}, \langle\delta b^\dagger\delta b\rangle_{\mathbf{q}}, \langle\delta b^2\rangle_{\mathbf{q}}, \langle\delta b^{\dagger 2}\rangle_{\mathbf{q}}, \langle\delta b^\dagger\delta b^2\rangle_{\mathbf{q}}, \langle\delta b^{\dagger 2}\delta b\rangle_{\mathbf{q}})$. We note that the fluctuation $\delta\langle\delta b\rangle_{\mathbf{q}}$ ($\delta\langle\delta b^\dagger\rangle_{\mathbf{q}}$) coincides with the fluctuation of the order parameter $\delta\psi_{\mathbf{q}}$ ($\delta\psi^*_{-\mathbf{q}}$). M can be easily diagonalized numerically revealing the spectrum in Fig. 3 (we display only the real part γ corresponding to damping). The lowest-lying branch gives $\gamma_{\mathbf{q}} < 0$ in an interval around $\mathbf{q} = 0$. This means that the correlation functions grow exponentially $\propto e^{\gamma t}$ in a range of low momenta, resulting in a long wavelength density wave.

Because of the scale separation for $\mathbf{q} \to 0$ in M apparent from Fig. 3, we can apply second order perturbation theory twice in a row to integrate out the fast modes $\gamma \propto \kappa$ and $\propto \kappa n$. We then obtain an effective low energy EOM for the fluctuations of the order parameter ($\delta\psi_{\mathbf{q}}$, $\delta\psi^*_{-\mathbf{q}}$), governed by a 2×2 matrix

$$M_{\text{eff}} = \begin{pmatrix} Un + \epsilon_{\mathbf{q}} - i\kappa_{\mathbf{q}} & Un + 9un\kappa_{\mathbf{q}} \\ -Un - 9un\kappa_{\mathbf{q}} & -Un - \epsilon_{\mathbf{q}} - i\kappa_{\mathbf{q}} \end{pmatrix}, \tag{6}$$

where $\epsilon_{\mathbf{q}} = J\mathbf{q}^2$ represents the kinetic contribution and $\kappa_{\mathbf{q}} = 2(2n+1)\kappa\mathbf{q}^2$ is the bare dissipative spectrum. The

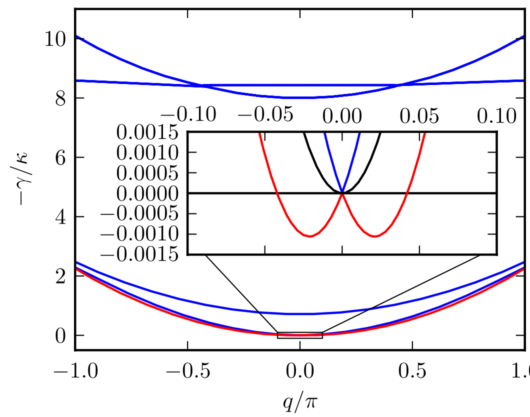

FIG. 3 (color online). Real (dissipative) part of the spectrum $\gamma_{\mathbf{q}}$ from the analytical low-density limit for $J = 0$, $n = 0.1$, and $U = 1.0\kappa$. The inset magnifies the parameter region with unstable modes (red solid line). The black solid line is the bare dissipative spectrum $\kappa_{\mathbf{q}}$.

form of the EOM reflects the structure of the spatial fluctuations which are included in our approach, that may be understood as scattering off the mean fields in opposite directions. We note that a naive *a priori* restriction to the 2×2 set corresponding to the subset $(\delta\psi_\ell, \delta\psi_\ell^*)$ would be inconsistent, for example, destroying the dark state property present in the correct solution $M_{\rm eff}$. On the other hand, factorizing the correlation functions in the Liouvillian $\mathcal{L}_\ell$ yields a dissipative Gross-Pitaevski equation but its linearization in time produces a matrix $M_{\rm eff}$ *without* the fluctuation induced term $\sim u$ and fails to describe the dynamical instability. Thus, to correctly capture the physics of the instability at $\mathbf{q} \to 0$, the onsite quantum correlations renormalizing $M_{\rm eff}$ have to be taken into account.

We can make the nature of the instability even more transparent calculating the lowest eigenvalue of $M_{\rm eff}$, $\gamma_{\mathbf{q}} \simeq ic|\mathbf{q}| + \kappa_{\mathbf{q}}$, with speed of sound $c = \sqrt{2Un[J - 9Un/(2z)]}$. If the hopping amplitude is smaller than the critical value $J_c = 9Un/(2z)$ the speed of sound turns imaginary and contributes to the dissipative real part of $\gamma_{\mathbf{q}}$. The nonanalytic renormalization contribution $\sim|\mathbf{q}|$ always dominates the bare quadratic piece for low momenta, explaining the shape in the inset of Fig. 3 and rendering the system unstable. The linear slope of the stability border for small J and U is clearly visible in Fig. 1. In summary, the origin of the instability is traced back to a subtle interplay of short time quantum and long wavelength classical fluctuations.

Conclusion.—The features found in the present model are expected to be generic and representative for a whole class of nonequilibrium models discussed recently in the context of reservoir engineering and dissipative preparation of given long-range ordered entangled states of qubits or spins on a lattice [18,19] and paired fermions [11,20].

We thank M. Hayn, A. Pelster, S. Kehrein, M. Möckel, and J. V. Porto for interesting discussions. This work was supported by the Austrian Science Foundation through SFB FOQUS, SCALA and by EU Networks.

[1] P. Calabrese and J. Cardy, Phys. Rev. Lett. **96**, 136801 (2006); C. Kollath, A. M. Läuchli, and E. Altman, *ibid.* **98**, 180601 (2007); A. Silva, *ibid.* **101**, 120603 (2008); M. Möckel and S. Kehrein, *ibid.* **100**, 175702 (2008).

[2] M. Greiner, O. Mandel, T. W. Hänsch, and I. Bloch, Nature (London) **419**, 51 (2002); B. Paredes *et al.*, *ibid.* **429**, 277 (2004); L. E. Sadler *et al.*, *ibid.* **443**, 312 (2006).

[3] M. Cramer, C. M. Dawson, J. Eisert, and T. J. Osborne, Phys. Rev. Lett. **100**, 030602 (2008); M. Rigol, V. Dunjko, and M. Olshanii, Nature (London) **452**, 854 (2008); G. Roux, Phys. Rev. A **79**, 021608 (2009); L. C. Venuti and P. Zanardi, Phys. Rev. A **81**, 032113(R) (2010).

[4] T. Kinoshita, T. Wenger, and D. S. Weiss, Nature (London) **440**, 900 (2006); S. Hofferberth *et al.*, Nature Phys. **4**, 489 (2008).

[5] S. Montangero, R. Fazio, P. Zoller, and G. Pupillo, Phys. Rev. A **79**, 041602(R) (2009); J. Schachenmayer, G. Pupillo, and A. J. Daley, New J. Phys. **12**, 025014 (2010).

[6] K. Sengupta, S. Powell, and S. Sachdev, Phys. Rev. A **69**, 053616 (2004); W. H. Zurek, U. Dorner, and P. Zoller, Phys. Rev. Lett. **95**, 105701 (2005); C. De Grandi, V. Gritsev, and A. Polkovnikov, Phys. Rev. B **81**, 012303 (2010).

[7] C. N. Weiler *et al.*, Nature (London) **455**, 948 (2008).

[8] S. A. Moskalenko and D. W. Snoke, *Bose-Einstein Condensation of Excitons and Biexcitons* (Cambridge University Press, Cambridge, England, 2000); J. Keeling, F. M. Marchetti, M. H. Szymanska, and P. B. Littlewood, Semicond. Sci. Technol. **22**, R1 (2007).

[9] E. G. Dalla Torre, E. Demler, T. Giamarchi, and E. Altman, arXiv:0908.0868.

[10] S. Sachdev, *Quantum Phase Transitions* (Cambridge University Press, Cambridge, England, 1999).

[11] S. Diehl *et al.*, Nature Phys. **4**, 878 (2008); B. Kraus *et al.*, Phys. Rev. A **78**, 042307 (2008).

[12] A. Aspect *et al.*, Phys. Rev. Lett. **61**, 826 (1988); M. Kasevich and S. Chu, *ibid.* **69**, 1741 (1992).

[13] B. Wu and Q. Niu, Phys. Rev. A **64**, 061603 (2001); A. Smerzi, A. Trombettoni, P. G. Kevrekidis, and A. R. Bishop, Phys. Rev. Lett. **89**, 170402 (2002); E. Altman *et al.*, *ibid.* **95**, 020402 (2005).

[14] S. Burger *et al.*, Phys. Rev. Lett. **86**, 4447 (2001); M. Cristiani *et al.*, Opt. Express **12**, 4 (2004); J. Mun *et al.*, Phys. Rev. Lett. **99**, 150604 (2007).

[15] J. Kasprzak *et al.*, Nature (London) **443**, 409 (2006); M. Wouters and I. Carusotto, arXiv:1001.0660.

[16] A. Schmid, Phys. Rev. Lett. **51**, 1506 (1983); S. Chakravarty, G.-L. Ingold, S. Kivelson, and A. Luther, *ibid.* **56**, 2303 (1986); A. Kampf and G. Schön, Phys. Rev. B **36**, 3651 (1987); S. Chakravarty, S. Kivelson, G. T. Zimanyi, and B. I. Halperin, *ibid.* **35**, 7256 (1987); R. Fazio and H. van der Zant, Phys. Rep. **355**, 235 (2001).

[17] C. W. Gardiner and P. Zoller, *Quantum Noise* (Springer-Verlag, Berlin, 1999).

[18] F. Verstraete, M. M. Wolf, and J. I. Cirac, Nature Phys. **5**, 633 (2009).

[19] H. Weimer *et al.*, Nature Phys. **6**, 382 (2010).

[20] W. Yi *et al.* (to be published).